ISSN 0031-918X, The Physics of Metals and Metallography, 2013, Vol. 114, No. 6, pp. 469–473. © Pleiades Publishing, Ltd., 2013.
Original Russian Text © M.V. Petrik, Yu.N. Gornostyrev, 2013, published in Fizika Metallov i Metallovedenie, 2013, Vol. 114, No. 6, pp. 514–518.

THEORY OF METALS

# Local Deformations and Chemical Bonding in Fe–$X$ ($X$ = Si, Al, Ga, Ge) Soft Magnetic Alloys

**M. V. Petrik[a, b] and Yu. N. Gornostyrev[b, c]**

[a] *Ural Federal University, ul. Mira 19, Ekaterinburg, 620002 Russia*
[b] *Institute of Quantum Materials Science, Ekaterinburg, Russia*
[c] *Institute of Metal Physics, Ural Branch, Russian Academy of Sciences, ul. S. Kovalevskoi 18, Ekaterinburg, 620990 Russia*
*e-mail: Mikhail.Petrik@iqms.ru*

Received September 21, 2012

**Abstract**—Dilute alloys based on ferromagnetic bcc iron modified by 3*p* (Al, Si) and 4*p* (Ga, Ge) elements are studied using the methods of the density-functional theory. It is shown that the local deformations and solution energies depend on the position of an alloying element in the periodic system. The nature of Fe–$X$ chemical bonding varies from weak metallic in Fe–Ga to strong quasi-covalent in Fe–Si, which determines the values of local deformations in these alloys. The formation of pairs of impurity atoms in the position of the next-nearest neighbors leads to tetragonal lattice deformations, the value of which is highest for Si and Ge. The role of local deformations in the formation of unusual magnetic properties of Fe–$X$ alloys is discussed.

*Keywords*: soft magnetic materials, iron alloys, short-range order, ab initio calculations
**DOI:** 10.1134/S0031918X13060112

## INTRODUCTION

Alloys based on bcc iron modified by Si, Al, Ga, and Ge with an impurity concentration close to the boundary of the two-phase field are widely used as soft magnetic materials. Fe–Si and Fe–Al alloys are characterized by high magnetic permeability and saturation magnetization. Their soft magnetic properties are substantially improved by heat treatment in a dc magnetic field or by mechanical loading due to induced (by an external action) magnetic anisotropy [1–4]. The Fe–Ga and Fe–Ge alloys are considered to be promising materials for actuators and sensors because of the great magnetostriction effect [5, 6]. The causes of the magnetoelastic behavior of these alloys differ, but, in all cases, the formation of a definite type of short-range chemical order (SRO) plays an important role [4, 7–9]. Moreover, local lattice deformations, which result from the presence of an impurity, play a prominent part in the formation of magnetic properties of these alloys [4, 10]; their value governs alloy restructuring under the effect of an external load.

The electronic structure and magnetic characteristics of Fe–$X$ alloys with a definite type of order of atoms of the alloying element $X$ have been studied in a number of works [3–5, 11]. However, little is known about local deformations that result from the presence of single impurities or their complexes (only work [3] is devoted to the study of the Fe–Si alloy). The value of the deformations is usually estimated based on the on the concentration-induced expansion of an alloy or on the results of a comparison of the ionic radii of the impurity and matrix, which, however, can lead to qualitatively incorrect conclusions [12].

In this work, α-Fe–$X$ ($X$ = Si, Al, Ga, Ge) alloys in the ferromagnetic state are studied by the methods of the electron-density-functional theory. Solution energies and values of local deformations in the vicinity of a single impurity and a pair of next-nearest-neighbor impurities are calculated. The results agree well with the known calculation and experimental data and make it possible to establish a relationship between the specific features of the electronic structure of the impurity and lattice deformations.

## CALCULATION METHOD

The electronic structure, local deformations, and the energy of the Fe–$X$ alloys were calculated by methods of the density-functional theory based on localized quasi-atomic orbitals (LCAO) using a SIESTA software package [13]. The applicability of this approach to iron alloys was substantiated in [14, 15]. It was shown in these works that the shrinkage of the basis set for 3*d* orbitals of Fe compared to commonly used DZ (double-ξ) and DZP (double-ξ-polarized) methods does not decrease the accuracy of calculations, but reduces computational expenditures as compared to the methods with a plane-wave basis.

**Table 1.** Lattice deformations induced by a dissolved element in a 128-atom cell. $\varepsilon_{loc}^{(1)}$ is the relative change in the distance between an impurity atom and an Fe atom on the first coordination shell (CS) coordination shell in the ⟨111⟩ direction; $\varepsilon_{loc}^{(2)}$ is the relative change in the distance between an impurity atom and an Fe atom on the second CS in the ⟨100⟩ direction; $\varepsilon_{tot}$ is the relative change in the supercell length in the ⟨100⟩ direction; $E_{sol}$ is the energy of solution of an impurity element; $R_i$ is the ionic radius of the dissolved element; $\Delta q$ is the charge transfer from an impurity atom to an iron atom calculated from an analysis of Mulliken populations [21]

| Parameters | Al | Si | Ga | Ge |
|---|---|---|---|---|
| $\varepsilon_{loc}^{(1)}$, % | 1.36 | 0.04 | 1.56 | 1.36 |
| $\varepsilon_{loc}^{(2)}$, % | −0.69 | −0.73 | −0.24 | −0.32 |
| $\varepsilon_{tot}$, % | −0.1 | 0.00 | −0.1 | −0.1 |
| $E_{sol}$, eV | −1.02 | −1.25 | −0.48 | −0.77 |
| $R_i$, Å | 0.53 | 0.39 | 0.62 | 0.44 |
| $\Delta q$, $e$ | 0.24 | 0.16 | 0.49 | 0.28 |

To describe the valence electrons of Fe, we used the DZ basis for 4*s* states and the SZ (single-ξ) basis for 4*p* and 3*d* states; the cutoff radius of the orbitals was selected to be 2.95 Å. For impurity atoms, the standard DZP basis was used. The core electrons were taken into account by using the norm-preserving pseudopotential constructed following the Troullier–Martins procedure [16]. The nonlocal components of the pseudopotential were presented following the Kleinman–Bylander procedure [17]. The exchange-correlation energy was taken into account in the GGA approximation with the Perdew–Burke–Ernzerhof parameterization (GGA-PBE) [18]. The calculations were carried out using 54 and 128 atomic cells that contain one or two impurity atoms. The cutoff energy was selected to be 600 Ry, and the networks of *k* points constructed following the Monkhorst–Pack procedure [19] were used with dimensions of $3 \times 3 \times 3$ in the case of the cell with 128 atoms and $6 \times 6 \times 6$, for the cell with 54 atoms. The full relaxation of ion positions and of the cell volume was implemented. The calculation accuracy was 0.02 eV/Å for forces and 1 meV for the total energy.

## CALCULATION RESULTS

The substitution of an alloying-element atom for a Fe atom results in local variations in the electronic structure and displacements of Fe atoms closest to the alloying-element atom from the equilibrium position. Table 1 presents calculated total deformations $\varepsilon_{tot}$ of a crystallite along principal crystallographic directions ⟨100⟩, as well as local deformations $\varepsilon_{loc}^{(1)}$ and $\varepsilon_{loc}^{(2)}$, which represent relative changes in the distances (the deformation value was determined with respect to the calculated lattice parameter of bcc Fe equal to 2.886 Å) from the impurity atom to the iron atoms on the first and second coordination shells (CSs). It follows from the data given in Table 1 that the deformations that result from the presence of impurities cannot be explained by the dimensional mismatch between the atoms of the dissolved elements and the matrix atoms. Indeed, the ionic radius $R_i$ for all impurities is less than for iron ($R_{Fe} = 0.83$ Å), while the deformations observed are $\varepsilon_{loc}^{(1)} \geq 0$.

The total deformation of the crystal $\varepsilon_{tot}$ is negative and has approximately the same value of −0.1% for all elements (at their concentrations $C_X \sim 0.8\%$) except for Si, for which $\varepsilon_{tot} = 0$. An increase in the concentration of the alloying elements to $C_X \sim 1.8\%$ (for the 54-atomic cell) leads to growth in $\varepsilon_{tot}$ for Al, Ga, and Ge to 0.26, 0.31, and 0.17%, respectively. For Si, $\varepsilon_{tot}$ remains unchanged. This specific feature of the Fe–Si alloy agrees with the results obtained earlier [20], where the authors found that, at a low Si concentration, no changes in the lattice parameter of the Fe–Si alloy occur. Thus, the results obtained show that, in the low concentration range, the behavior of the alloys under study does not obey Vegard's law, i.e., $\varepsilon_{tot}$ either is equal to zero or changes its sign with increasing $C_X$.

The values of the local deformations $\varepsilon_{loc}$ regularly change depending on the position of a dissolved element in the periodic system. It can be seen from Table 1 that the mode of displacements of Fe atoms on the first ($\varepsilon_{loc}^{(1)}$) and second ($\varepsilon_{loc}^{(2)}$) CSs, as well as the solution energy $E_{sol}$, are determined by either the impurity atoms belong to the 3*p* (Al, Si) or 4*p* (Ga, Ge) groups of elements, i.e., by the specific features of their electronic structure. This is especially clearly seen when comparing the values of $\varepsilon_{loc}^{(2)}$ and $E_{sol}$ for various alloys from Table 1 (note that the value of $E_{sol}$ for Si agrees well with the value obtained earlier in [1] by using Q-Espresso). The mode of changes in $E_{sol}$ is indicative of the fact that the 3*p* elements form stronger chemical bonding with Fe atoms than the 4*p* elements. Moreover, within each period, $E_{sol}$ decreases with an increasing number of electrons in the *p* shell, which evinces the strengthening of the Fe–*X* bonding. This is the cause of a regular variation in the distance between impurity atoms and atoms of the first or second CSs of iron with increasing number of *p* electrons (Table 1). Among the elements under consideration, Si forms the strongest bonds with Fe atoms, which leads to the specific features of local deformations it induces.

Chemical bonds between iron and impurity atoms in the alloys under study are formed as a result of the hybridization of *p*–X and *d*–Fe states and depend on

the number of valence $p$ electrons. As the number of $p$ electrons grows, the degree of covalence of bonding increases. An isolated impurity with a single $p$ electron (Al, Ga) forms metallic bonding with iron atoms, whereas isolated impurities with two $p$ electrons (Si, Ge) form quasi covalent bonds [22, 23]. This follows from an analysis of the local densities of states (LDOS) shown in the figure. For Al, no signs of $p$–$d$ hybridization are found in the LDOS, while they are clearly seen for Si as peaks in the energy range from –7 to –5 eV. A similar difference is observed when comparing LDOS for the Fe–Ga and Fe–Ge alloys. An increase in the degree of covalence of bonding is also confirmed by the calculated values of the charge transfer $\Delta q$ from the impurity to the $d$ conduction band of iron, which decrease with increasing number of $p$ electrons (Table 1).

The difference in chemical bonding formed by 3$p$ and 4$p$ elements with iron is due to many factors, among which the degree of spatial locality of 3$p$ and 4$p$ orbitals is the most significant. The electronic states that correspond to 3$p$ orbitals are more localized; therefore, the 3$p$ elements form more covalent bonds with iron atoms of the first CS. As was mentioned above, this results in the stronger bonding of 3$p$ elements with Fe atoms than bonding of 4$p$ elements with Fe atoms. Thus, in the alloys under consideration, the nature of bonding with Fe changes from weak metallic in Fe–Ga to strong quasi-covalent in Fe–Si despite the close positions of the alloying elements in the periodic system.

As was mentioned in the introduction, the existence of a definite chemical short-range order plays an important role in the formation of magnetic properties of the alloys under consideration. In particular, it has been shown that the formation of pairs of impurity atoms in the position of the second neighbors is significant for the appearance of induced magnetic anisotropy [4, 9]. Table 2 presents the results of calculations of the local and total deformations in a cell containing a pair of impurity atoms in the position of the second neighbors. The lattice distortions in the vicinity of a pair of impurity atoms are determined by the balance of Fe–$X$ and $X$–$X$ interactions. It can be seen from Table 2 that the relative change in the distance between the impurity atoms is positive ($\varepsilon_{loc}^{X-X} > 0$) for all of the alloying elements under consideration; therefore, it should be expected that the $X$–$X$ interaction is weaker than the Fe–$X$ interaction. The value of $\varepsilon_{loc}^{Al-Al}$ is minimum; this may be related to the closeness of the characteristic length of the Al–Al bond and $a_{Fe}$, while the lengths of $X$–$X$ bonds for the remaining dissolved elements are considerably shorter (Table 2). The obtained value of $\varepsilon_{loc}^{X-X}$ for the Ga–Ga pair agrees well with the measured value [24].

Just as in the case of an isolated impurity, the local deformations induced by a pair of impurity atoms change regularly within each period with increasing number of $p$ electrons of the dissolved element. A high degree of covalence of the Fe–Si and Fe–Ge bonds leads to a more pronounced tetragonality $c/a_{loc}$ of the local environment of these pairs as compared to Fe–Al and Fe–Ga. The high local deformations induced by an impurity pair are compensated for by displacements of Fe atoms on the next coordination shells such that the total tetragonality $c/a_{tot}$ of the supercell proves to be substantially less than its local value. It can be seen from Table 2 that the value of $c/a_{tot}$ is small for the Fe–Si and Fe–Ge alloys and is the highest for the Fe–Ga alloy. It should be noted that the total tetragonality of the supercell depends strongly on the concentration and location of the impurities. The maximum

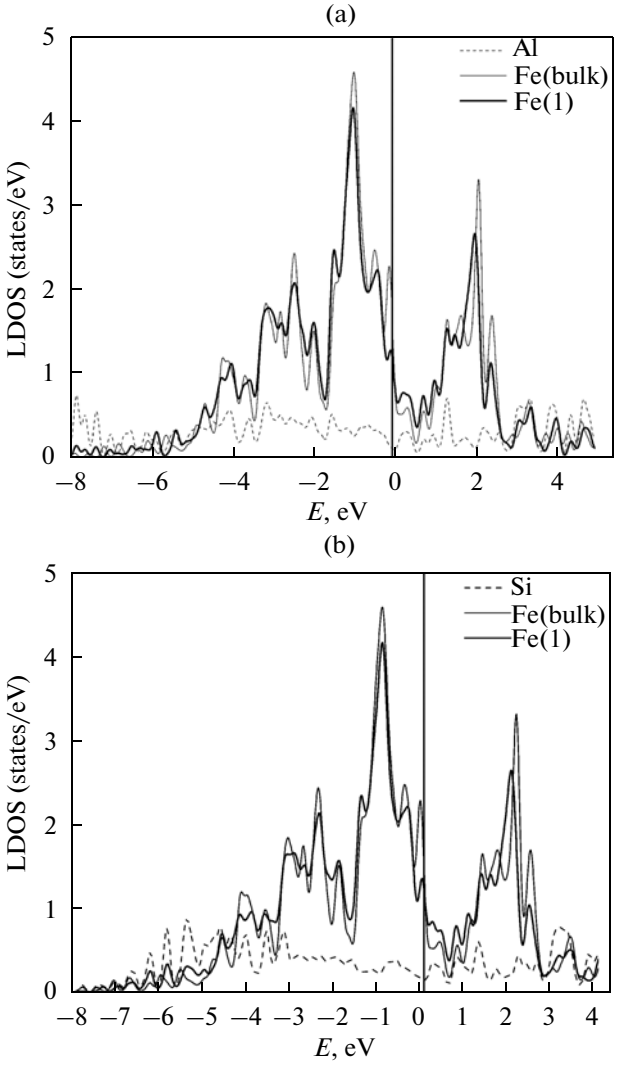


Diagrams of the local density of electronic states (LDOS) for (a) Fe–Al and (b) Fe–Si alloys; the dashed lines correspond to the LDOS on a Si (Al) impurity atom; thin solid lines, to the LDOS on an Fe atom far from an impurity atom; and thick solid lines, to the LDOS on an Fe atom in the first CS.

**Table 2.** Lattice deformations induced by a pair of dissolved elements located in the positions of second neighbors in a 128-atom cell. $\varepsilon_{loc}^{X-X}$ is the relative change in the distance between impurity atoms as compared to $a_{Fe}$; $\varepsilon_{loc}^{Fe(1.2)-Fe(1.2)}$ is the relative change in the distance between Fe(1.2) atoms the first CS of which contains two impurity atoms; $\varepsilon_{loc}^{Fe(2)-X}$ is the relative change in the distance between the atoms of the second CS (Fe(2)) and the impurity atom; $c/a_{tot}$ is the coefficient of tetragonality of the supercell; and $c/a_{loc}$ is the coefficient of tetragonality of a local environments of an atomic pair

| Parameters | Al | Si | Ga | Ge |
|---|---|---|---|---|
| $\varepsilon_{loc}^{X-X}$, % | 2.23 | 7.84 | 5.07 | 7.03 |
| $\varepsilon_{loc}^{Fe(1.2)-Fe(1.2)}$, % | 2.18 | −2.47 | 2.07 | 0.49 |
| $\varepsilon_{loc}^{Fe(2)-X}$, % | −2.00 | −4.50 | −2.21 | −3.70 |
| $c/a_{tot}$, % | −0.12 | 0.05 | 0.16 | −0.03 |
| $c/a_{loc}$, % | 4.31 | 12.92 | 7.44 | 11.12 |
| Bond length, Å | 2.79 | 2.35 | 2.45 | 2.45 |

value of the tetragonality of the supercell is achieved at an ordered codirectional arrangement of pairs of impurities in the position of the second neighbors; this maximum value can be estimated from the data given in Table 2.

## CONCLUSIONS

The calculation results show that the impurity-induced disturbances in the iron lattice (changes in the electronic structure; local deformations), as well as the energy of an impurity dissolution, change regularly depending on the position of the impurity element in the periodic system. The nature of bonding that is formed between impurity atoms and the closest iron atoms varies from a weak metallic bonding in Fe–Ga to strong quasi-covalent in Fe–Si, which determines the specific features of local deformations in the vicinity of impurity atoms. In particular, the local deformations in the first CS in the vicinity of a Si atom are close to zero, which results from the equilibrium of forces of the Fe–Si and Fe–Fe bonds. The deformations $\varepsilon_{loc}^{(1)}$ in the Fe–Al alloy are substantially higher than those in the Fe–Si alloy due to a lesser covalence of Fe–Al bonding. The total deformation $\varepsilon_{tot}$ considerably differs from the deformations induced by the impurity in the nearest coordination shells. Therefore, based on the data on only the concentration-induced expansion, one cannot obtain information on the local deformations. The calculated deviation from Vegard's law can be attributed to the transformation of the electronic structure with increasing alloying-element concentration, which plays a significant role in the properties of these alloys [25].

The local deformations in the vicinity of a pair of impurities substantially exceed the total lattice distortions. The presence of Si–Si and Ge–Ge pairs in the Fe–$X$ alloy in the position of the second neighbors leads to strong local tetragonal distortions of their environment; therefore, the ordering of these pairs under the effect of an external load can be expected. It is generally agreed that this leads to an increase in the magnetic anisotropy during thermomechanical treatment, which was comprehensively studied in the Fe–Si alloy [1, 2]. One might expect that the Fe–Ge alloy can possess these properties, but we do not know any works on the study of the induced magnetic anisotropy in this alloy. The value of $c/a_{tot}$ is the highest for the Fe–Ga alloy, which demonstrates large magnetostriction. However, this characteristic has the lowest absolute value for the Fe–Ge alloy, while the lowest magnetostriction value is observed in the Fe–Si alloy [5]. Thus, the magnitude of $c/a_{tot}$ cannot serve as a parameter responsible for the magnetostriction value. In order to correctly describe it, the spin-orbital interaction should be allowed for; it cannot be considered in the context of the nonrelativistic approach that we use. Moreover, the maximum magnetostriction value is achieved in these alloys at fairly high concentrations of impurities and cannot be adequately described by the model of isolated pairs. The solution of the problem of short-range order formation requires the knowledge of effective interactions between the alloying elements; this problem will be discussed in the next work.

## ACKNOWLEDGMENTS

This work was supported in part by the Russian Foundation for Basic Research project no. 10-02-100435) and by the Presidium of the Russian Academy of Sciences (project no. 12-P-23-2005).

## REFERENCES

1. Y. Yoshizawa, S. Oguma, and K. Yamauchi, "New Fe-based soft magnetic alloys composed of ultrafine grain structure," J. Appl. Phys. **64**, 6044–6046 (1988).
2. B. Hofman and H. Kronmuller, "Stress-induced magnetic anisotropy in nanocrystalline FeCuNbSiB alloy," J. Magn. Magn. Mater. **152**, 91–98 (1996).
3. A. R. Kuznetsov, Yu. N. Gornostyrev, N. V. Ershov, V. A. Lukshina, Yu. P. Chernenkov, and V. I. Fedorov, "Atomic displacements and short-range order in the FeSi soft magnetic alloy: Experiment and ab initio calculations," Phys. Solid State **49**, 2290–2297 (2007).
4. O. I. Gorbatov, A. R. Kuznetsov, Yu. N. Gornostyrev, A. V. Ruban, N. V. Ershov, V. A. Lukshina, Yu. P. Chernenkov, and V. I. Fedorov, "Role of magne-

tism in the formation of a short-range order in iron–silicon alloys," J. Exper. Theor. Phys. **112**, 848–859 (2011).

5. J. B. Restorff, M. Wun-Fogle, K. B. Hathaway, A. E. Clark, T. A. Lograsso, and G. Petculescu, "Tetragonal magnetostriction and magnetoelastic coupling in Fe–Al, Fe–Ga, Fe–Ge, Fe–Si, Fe–Ga–Al and Fe–Ga–Ge alloys," J. Appl. Phys. **111**, 023905 (2012).
6. E. M. Summers, T. A. Lograsso, and M. Wun-Fogle, "Magnetostriction of binary and ternary Fe–Ga alloys," J. Mater. Sci. **42**, 9582–9594 (2007).
7. R. Wu, "Origin of large magnetostriction in FeGa alloys," J. Appl. Phys. **91**, 7358–7360 (2002).
8. J. Boisse, H. Zapolsky, and A. G. Khachaturyan, "Atomic scale modeling of nanostructure formation in Fe–Ga alloys with giant magnetostriction: Cascade ordering and decomposition," Acta Mater. **59**, 2656–2668 (2011).
9. O. I. Gorbatov, Yu. N. Gornostyrev, A. R. Kuznetsov, and A. V. Ruban, "Effect of magnetism on short-range order formation in Fe–Si and Fe–Al alloys," Solid State Phenom. **172–174**, 618–623 (2011).
10. M. L. Néel, "Anisotropie magnetique superficielle et surstructures d'orientation," J. Phys. Radiat. **15**, 225–239 (1954).
11. D. Wu, Q. Xing, R. W. McCallum, and T. A. Lograsso, "Magnetostriction of iron–germanium single crystals," J. Appl. Phys. **103**, 07B307 (2008).
12. M. A. Krivoglaz, *X-ray and Neutron Diffraction in Nonideal Crystals* (Springer, Berlin, 1996).
13. J. M. Soler, E. Artacho, J. D. Gale, A. Garcia, J. Junquera, P. Ordejón, and D. Sanchez-Portal, "The SIESTA method for ab initio order-*N* materials simulation," J. Phys.: Condens. Matter **14**, 2745 (2002).
14. R. Soulairol, C. C. Fu, and C. Barreteau, "Structure and magnetism of bulk Fe and Cr: From plane waves to LCAO methods," J. Phys.: Condens. Matter **22**, 295502 (2010).
15. C. C. Fu, F. Willaime, and P. Ordejon, "Stability and mobility of mono- and di-interstitials in α-Fe," Phys. Rev. Lett. **92**, 175503 (2004).
16. N. Troullier and J. L. Martins, "Efficient pseudopotentials for plane-wave calculations," Phys. Rev. B: Condens. Matter **43** (3), 1993–2006 (1991).
17. L. Kleinman and D. M. Bylander, "Efficacious form for model pseudopotentials," Phys. Rev. Lett. **48**, 1425–1428 (1982).
18. J. P. Perdew, K. Burke, and M. Ernzerhof, "Generalized gradient approximation made simple," Phys. Rev. Lett. **77**, 3865–3868 (1996).
19. H. J. Monkhorst and J. D. Pack, "Special points for Brillouin-zone integrations," Phys. Rev. B: Solid State **13**, 5188–5192 (1976).
20. N. I. Kulikov, D. Fristot, A. Postnikov, and J. Hugel, "Infuence of disorder on electronic structure and magnetic properties in Fe-rich Fe–Si alloys," Comp. Mater. Sci. **17**, 196–201 (2000).
21. R. S. Mulliken, "Electronic population analysis on LCAO-MO molecular wave functions," J. Chem. Phys. **23**, 1833–1831 (1955).
22. K. A. Mader, H. Kanel, and A. Baldereschi, "Electronic structure and bonding in epitaxially stabilized cubic iron silicides," Phys. Rev. B: **48**, 4364–4372 (1993).
23. A. Collins, R. C. O'Handley, and K. H. Johnson, "Bonding and magnetism in Fe–*M* (*M* = B, C, Si, N) alloys," Phys. Rev. B: Condens. Matter **38**, 3665–3670 (1988).
24. S. Pascarelli, M. P. Ruffoni, R. S. Turtelli, F. Kubel, and R. Grossinger, "Local structure in magnetostrictive melt-spun $Fe_{80}Ga_{20}$ alloys," Phys. Rev. B: Condens. Matter Mater. Phys. **77**, 184406 (2008).
25. T. Khmelevska, S. Khmelevskyi, A. V. Ruban, and P. Mohn, "Magnetism and origin of non-monotonous concentration dependence of the bulk modulus in Fe-rich alloys with Si, Ge and Sn: A first-principles study," J. Phys.: Condens. Matter **18**, 6677 (2006).

*Translated by D. Tkachuk*